Insights into regulation of human Schwann cell proliferation by Erk1/2 via a MEK-independent and p56Lck-dependent pathway from leprosy bacilli

Nikos Tapinos and Anura Rambukkana*

Laboratory of Bacterial Pathogenesis and Immunology, The Rockefeller University, Bronk Building Room 501, 1230 York Avenue, New York, NY 10021

Edited by Stanley Falkow, Stanford University, Stanford, CA, and approved May 11, 2005 (received for review February 11, 2005)

Activation of extracellular signal-regulated kinase (Erk) 1/2, which plays a critical role in diverse cellular processes, including cell proliferation, is known to be mediated by the canonical Raf-mitogen-activated protein kinase kinase (MEK) kinase cascade. Alternative MEK-independent signaling pathways for Erk1/2 activation in mammalian cells are not known. During our studies of human primary Schwann cell response to long-term infection of *Mycobacterium leprae*, the causative organism of leprosy, we identified that intracellular *M. leprae* activated Erk1/2 directly by lymphoid cell kinase (p56Lck), a Src family member, by means of a PKCε-dependent and MEK-independent signaling pathway. Activation of this signaling induced nuclear accumulation of cyclin D1, G_1/S-phase progression, and continuous proliferation, but without transformation. Thus, our data reveal a previously unknown signaling mechanism of glial cell proliferation, which might play a role in dedifferentiation as well as nerve regeneration and degeneration. Our findings may also provide a potential mechanism by which an obligate intracellular bacterial pathogen like *M. leprae* subverts nervous system signaling to propagate its cellular niche for colonization and long-term bacterial survival.

cell signaling | cell cycle | peripheral nerve | human | *Mycobacterium leprae*

Schwann cell proliferation is crucial for the development of the peripheral nervous system, nerve regeneration and degeneration, and tumorigenesis (1–3). However, much less is known about the signaling mechanisms that regulate Schwann cell proliferation. Among the cell signaling cascades, activation of extracellular signal-regulated kinase (Erk) 1 and Erk2 signaling play a critical role in cell proliferation (4, 5). The activation of Erk1/2 in response to extracellular cues, such as growth factors, requires phosphorylation by mitogen-activated protein kinase kinase (MEK) 1/2 by means of Raf family kinases, and MEK1/2 are the only known activators of Erk1/2 (4–6). No alternative MEK1/2-independent signaling pathways that activate Erk1/2 in mammalian cells have been described.

We have shown that myelinating and nonmyelinating Schwann cells display distinct functional responses to infection with *Mycobacterium leprae*, the causative organism of leprosy, and cell proliferation is a common feature during infection (7–9). Subsequent to infection, *M. leprae* preferentially invade human nonmyelinating Schwann cells and maintain long-term intracellular bacterial survival, which eventually leads to irreversible immune-mediated peripheral nerve damage, the hallmark of leprosy (10–14). One key to the pathogenic potential of *M. leprae* survival lies in the ability of this extremely slow-growing and strictly obligate intracellular bacterium to propagate its preferred niche so that sufficient Schwann cells are available for bacterial residence, survival, and replication (7, 8, 13). Using highly purified primary human Schwann cells, which mimic nonmyelinating phenotype-like Schwann cells, we found that *M. leprae* have the capacity to induce Schwann cell proliferation from inside the cells several weeks after infection. Because mammalian cell proliferation is defined as the increase in cell number resulting from completion of the cell division cycle in response to extracellular signals (15), we investigated the signaling mechanisms by which intracellular *M. leprae* regulate human Schwann cell cycle and proliferation.

Materials and Methods

Isolation, Purification, and Characterization of Human Primary Schwann Cells. Human Schwann cells were isolated from peripheral nerve tissues (provided by Patrick Wood, University of Miami, through the Organ Procurement Organization, Miami), which consisted of nerve roots making up the cauda equina (16). (See *Supporting Materials and Methods*, which is published as supporting information on the PNAS web site, for detailed procedures.)

Infection of human Schwann cells with *in vivo* grown *M. leprae* was carried out as described in refs. 7 and 9. *M. leprae* used in this study were derived from the footpads of athymic *nu/nu* mice (17) and were provided by J. L. Krahenbuhl (National Hansen's Disease Programs Laboratory, Baton Rouge, LA).

Gene Array and Real-Time Quantitative RT-PCR (TaqMan) Analyses. Human genome Affymetrix (Santa Clara, CA) GeneChips were used to determine differential cell cycle gene expression in human primary Schwann cells in response to intracellular *M. leprae*. For real-time RT-PCR, primers and fluorescently labeled probes from the coding regions of human cell cycle regulators were designed by using VECTOR NTI software (Invitrogen). Experimental details of gene array and real-time PCR are described in *Supporting Materials and Methods.*

RT-PCR, electron microscopy, antibodies, immunofluorescence, Western blot analysis, proliferation assays (BrdUrd uptake), pharmacological inhibition of kinases, kinase activity assays, cell cycle FACS analysis, transformation assays, and transfection experiments are all detailed in *Supporting Materials and Methods*.

Results and Discussion

Schwann cells serve as a reservoir for *M. leprae* after peripheral nervous system infection (7, 8, 10, 11). To recapitulate the fate of human Schwann cells in response to long-term intracellular residence of *M. leprae in vivo*, we isolated adult Schwann cells from peripheral nerves from different human donors, and each isolate was purified to homogeneity by FACS sorting using mAbs against neurotrophin receptor p75 as a marker for Schwann cells (18), and further characterized (Fig. 6, which is published as supporting information on the PNAS web site). These Schwann cells efficiently engulfed *M. leprae* (Fig. 1 *A–C*) and are functionally similar to nonmyelinating-like phenotypes (7).

This paper was submitted directly (Track II) to the PNAS office.

Abbreviations: Erk, extracellular signal-regulated kinase; MEK, mitogen-activated protein kinase kinase; DNM, dominant-negative mutant; PI3K, phosphatidylinositol 3-kinase; MEKI, MEK inhibitor; PI3KI, PI3K inhibitor; PKCI, PKC pan-inhibitor; Lck, lymphoid cell kinase; LckI, Lck inhibitor.

*To whom correspondence should be addressed. E-mail: rambuka@imap.rockefeller.edu.

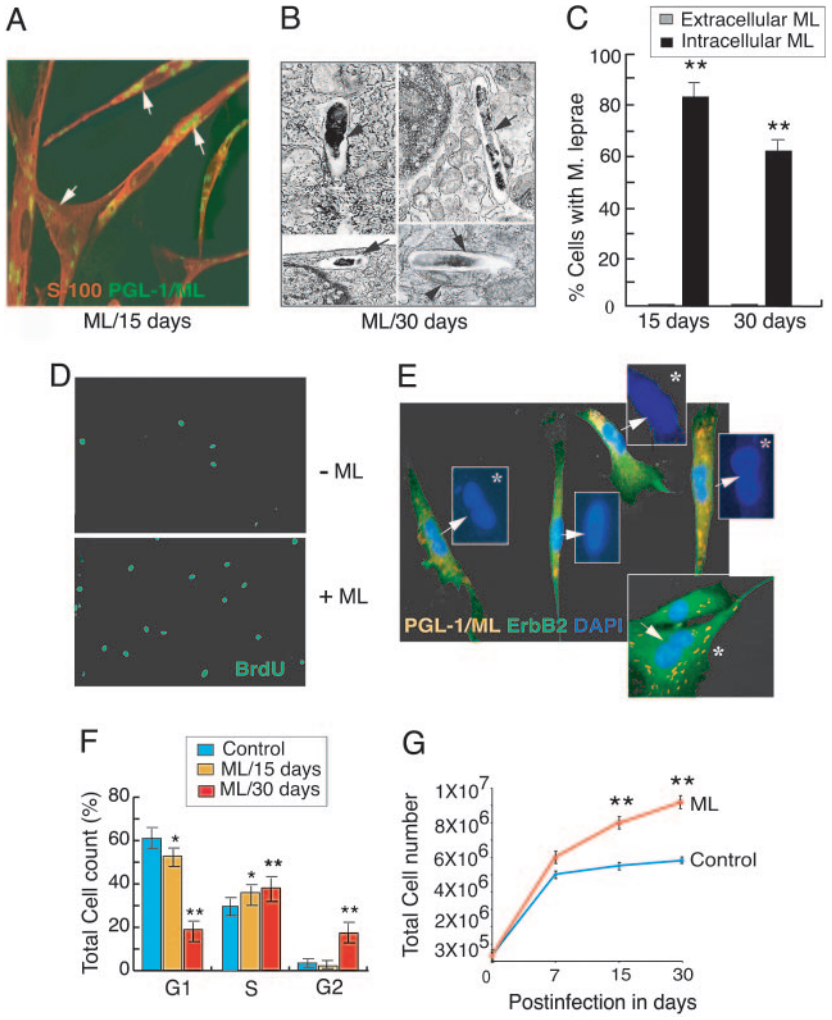

Fig. 1. Intracellular *M. leprae* promote Schwann cell cycle progression and proliferation. (*A–C*) Intracellular localization of *M. leprae* (ML) in purified primary human Schwann cells after 15 (*A*) and 30 (*B*) days of infection as determined by immunofluorescence and electron microscopy. In *A*, Schwann cell marker S-100 is red, and *M. leprae*-specific PGL-1 is green (indicated by the arrows). *B* shows electron microscopy. (*C*) Quantification of Schwann cells harboring intracellular *M. leprae*. **, $P < 0.001$, Student's *t* test. (*D*) BrdUrd uptake of *M. leprae*-infected (+ML) and control (−ML) Schwann cells. (*E*) Division of cell nuclei of infected cells as determined by DAPI labeling (*Insets*). Cells are double-stained with antibodies to ErbB2 (green) and PGL-1 (red/yellow). Asterisks in *Insets* show the dividing nuclei (arrows). (*F*) Cell cycle distribution of asynchronously growing *M. leprae*-infected human Schwann cells as analyzed by FACScan using propidium iodide. The percentage of total cells in G_1, S, and G_2 phases of the cell cycle are shown. The data are from three individual experiments from Schwann cells purified from two different organ donors. *, $P < 0.005$; **, $P < 0.001$, Student's *t* test. (*G*) Total Schwann cell counts from asynchronized cultures before (day 0; starting with equal cell numbers) and 7, 15, and 30 days after *M. leprae* infection are shown from four individual experiments. **, $P < 0.0005$, Student's *t* test.

We maintained infected primary cultures up to 15 and 30 days (in some cases up to 40 days) and demonstrated bacterial presence exclusively inside Schwann cells (Fig. 1 *A–C* and *E*). Strikingly, human Schwann cells that harbor intracellular *M. leprae* showed increased cell proliferation. Infected cells with numerous *M. leprae* showed a significant increase in uptake of BrdUrd (5-bromodeoxyuridine), which represents S-phase cells (Fig. 1*D*), and in the division of cell nuclei, which represents mitosis (Fig. 1*E* and *Insets*). The infected cells exhibited no signs of apoptosis or cytopathic effects (Fig. 7, which is published as supporting information on the PNAS web site). Cell cycle FACS analysis revealed that the total cell count in G_1 phase of 30-day-infected Schwann cells was significantly reduced compared with controls, whereas infected cells, particularly in G_2 phase, were dramatically increased (Fig. 1*F*). This finding suggests that intracellular *M. leprae* accelerated G_1 phase progression with earlier S-phase entry and that significant numbers of cells have entered G_2 phase. In agreement with these results, we found a significant increase of the total number of infected cells 15 and 30 days after infection ($P < 0.0001$), and ≈60% of Schwann cells at 30 days still harbored considerable numbers of *M. leprae* (Fig. 1*C*). Thus, we concluded that cell cycle progression and proliferation are due to Schwann cell response to long-term residence of intracellular *M. leprae*.

To begin to address how intracellular *M. leprae* modulate the human Schwann cell cycle, we used Affymetrix human GeneChips to identify key cell cycle genes. Among the differentially expressed cell cycle genes, and on the basis of relative gene expression by >2-fold criteria (Affymetrix DATA MINING TOOL 3.0 software), it was found that cyclin D1 and p21, two of the key G_1 phase cell cycle regulators (19), were significantly up-regulated at day 30 but not at day 3 or 7 (Fig. 2*A*). Because three separate gene array experiments with 30-day-infected Schwann cells from two different organ donors confirmed these findings (Fig. 2*B*), we focused most of our subsequent studies on day 30 postinfection. We further validated gene array data by performing real-time quantitative RT-PCR (TaqMan, Applied Biosystems) using specific primer/probe combinations for human cyclin D1 and p21 (Fig. 2*C*). Together, these results suggest that intracellular *M. leprae*, after long incubation (30 days), induce cyclin D1 and p21 gene transcription in human Schwann cells.

Consistent with gene expression data, total cyclin D1 protein was significantly up-regulated in 30-day-infected cells in asynchronized cultures (Fig. 2*D*). However, there was no change in expression of p21 protein despite the up-regulation of p21 gene at day 30. The reason for the lack of increase in p21 protein with up-regulated p21 mRNA transcript is currently unclear. Hence, we focused our studies on cyclin D1 and examined the role of Erk1/2 signaling in *M. leprae* regulation of cyclin D1 on the basis of increased Erk1/2 phosphorylation in 30-day-infected cells (Fig. 2*D*).

Modulating the abundance of cyclin D1 is one means by which cells control their progression through G_1 phase of the cell cycle and subsequent proliferation (15, 19, 20). To test the direct role of cyclin D1 in *M. leprae*-induced cell cycle progression, 30-day-infected and control primary human Schwann cells were transiently transfected with a dominant-negative mutant (DNM) of cyclin D1 (T156A with

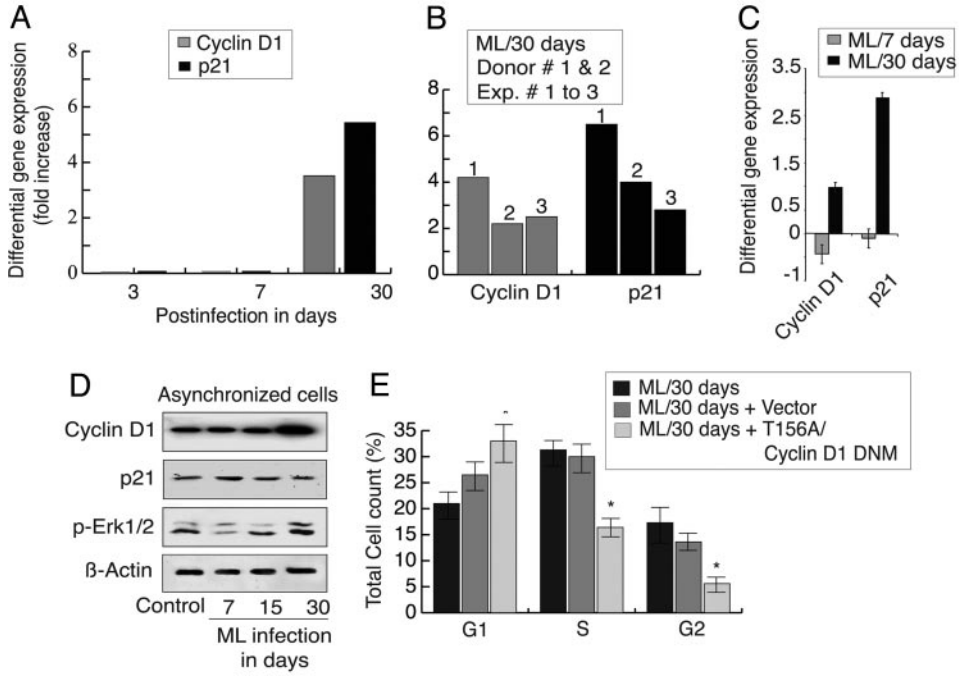

Fig. 2. Intracellular *M. leprae* induce cyclin D1 gene and protein expression in human Schwann cells; role in G_1/S-phase progression is shown. (*A* and *B*) Fold increase of differentially expressed cyclin D1 and p21 genes in *M. leprae*-infected Schwann cells as analyzed by using Affymetrix human GeneChips. (*A*) Differentially expressed cyclin D1 and p21 genes in asynchronized Schwann cells at postinfection day 3, 7, and 30. (*B*) Cyclin D1 and p21 gene expression in 30-day-infected Schwann cells from three individual experiments (experiments are labeled 1–3) ($P < 0.001$). (*C*) Quantitative real-time PCR analysis of cyclin D1 and p21 genes in human Schwann cells 7 and 30 days after *M. leprae* infection. Differentially expressed genes are presented after normalization with GAPDH gene expression relative to control expression. (*D*) Protein levels of cyclin D1 and p21 and phosphorylation of Erk1/2 from asynchronized cultures of human primary Schwann cells infected with *M. leprae*. Expression was measured by Western blot analysis of total cell extracts using antibodies to cyclin D1, p21, and phospho-specific (p) Erk1/2. (*E*) Overexpression of the T156A cyclin D1 DNM decreased the G_1 phase progression of *M. leprae*-infected Schwann cells. Cell cycle FACS analysis of 30-day-infected human primary Schwann cells transfected with vector alone and T156A/cyclin D1 DNM. Data are from three independent cell cycle FACS experiments showing the mean percentage of cell population in G_1, S, and G_2 phases. *, $P < 0.005$, Student's *t* test.

N-terminal FLAG; Fig. 8, which is published as supporting information on the PNAS web site). T156A expression is known to prevent nuclear accumulation of cyclin D1 and induce cell cycle arrest by blocking G_1 phase progression (21). The overexpression of the cyclin D1 DNM in 30-day-infected Schwann cells reversed the effects of intracellular *M. leprae* on Schwann cell cycle progression (Fig. 2*E*). G_1 population was significantly increased with a concomitant decrease in S and G_2 populations in 30-day-infected/T156A transfected cells, suggesting that functional blockade of cyclin D1 is sufficient to abolish G_1/S-phase progression in Schwann cells induced by intracellular *M. leprae*.

The regulation of cyclin D1 and subsequent G_1 phase progression require the participation of multiple signaling pathways, which include Erk1/2 and phosphatidylinositol 3-kinase (PI3K) signaling that are normally activated by binding of growth factors and extracellular matrix proteins to receptor tyrosine kinase and integrins, respectively (19, 22, 23). Because the observed cyclin D1 up-regulation in infected Schwann cells is a consequence of cellular response to intracellular *M. leprae* (Fig. 1*C*), we examined whether Erk1/2 signaling can be activated by *M. leprae* from inside the cells as an intracellular cue. Even after complete removal of serum and heregulin-1β, a potent Schwann cell mitogen that activates Erk1/2 by means of the Ras/Raf/MEK pathway in primary cultures (24), infected cells showed a significant phosphorylation of Erk1/2 compared with controls (Fig. 3*A*).

If intracellular *M. leprae* use canonical growth factor-activated SOS/Ras/Raf/MEK (or PI3K/Akt) pathways to phosphorylate Erk1/2 (for example, by inducing the release of Schwann cell growth factors by an autocrine pathway), specific inhibition of SOS and MEK (or PI3K) should block downstream phosphorylation of Erk1/2 (22–25). We have used well characterized pharmacological inhibitors U0126 and LY294002, which are specific for MEK1/2 and PI3K, respectively [MEK inhibitor (MEKI) and PI3K inhibitor (PI3KI), respectively] (22–24). Despite serum starvation and continuous presence of U0126 and LY294002 for 48 h, phosphorylation of Erk1/2 was not inhibited in infected Schwann cells (Fig. 3*B*). Similar pErk1/2 activation was detected with U0126 alone (data not shown). As expected, phosphorylation of MEK1/2 was inhibited in both controls and infected cells (Fig. 3*B*). In addition, treatment of synchronized infected Schwann cells with SOS-inhibitory peptide, which abolishes the upstream Ras-dependent Erk1/2 signaling (25), also failed to inhibit the phosphorylation of Erk1/2 in infected Schwann cells (Fig. 3*B*). In contrast, heregulin-1β-induced activation of Erk1/2, which is mediated by the Ras, Raf, and MEK1/2 pathways in Schwann cells (24), is markedly inhibited by U0126 and SOS inhibitors (data not shown). We then examined the capacity of activated cellular Erk1/2 to phosphorylate its downstream target transcription factor, Elk-1. Active Erk1/2 immunoprecipitated from infected synchronized Schwann cells in the presence of inhibitors produced significantly higher phosphorylation of Elk-1 compared with noninfected Schwann cells (Fig. 3*C*), further suggesting the ability of *M. leprae* to induce Erk1/2 kinase activity independent of the MEK1/2 pathway.

We next examined the role of *M. leprae*-induced Erk1/2 signaling in G_1/S-phase regulation by transiently transfecting cells with a $p44^{mapk}$ DNM T192A (23). Infected Schwann cells transfected with T192A showed a significant reduction in total cyclin D1 protein expression and in S-phase population compared with cells transfected with an empty vector ($P < 0.001$) (Fig. 3*D*), suggesting the direct involvement of *M. leprae*-induced Erk2 in cyclin D1 expression and S-phase entry of infected cells.

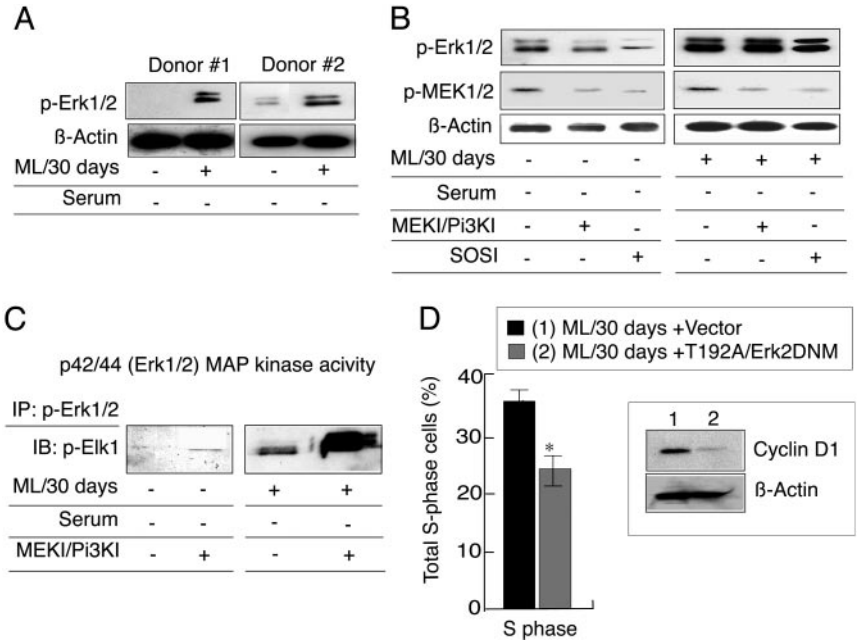

Fig. 3. Role of MEK-independent Erk1/2 signaling in *M. leprae*-induced cyclin D1 and G_1/S-phase progression. (*A–C*) Intracellular *M. leprae* activate Erk1/2 by means of MEK/PI3K-independent pathways. (*A*) Total lysates of 30-day-infected human Schwann cells purified from two different organ donors were synchronized for 48 h and then blotted with anti-phospho-Erk1/2 antibody. (*B*) Thirty-day-infected and control cells were synchronized for 48 h in the continuous presence of MEKI UO126 and PI3KI LY294002, and SOS inhibitory peptide (SOSI) and cell lysates were blotted with antibody to phospho-Erk1/2 and phospho-MEK1/2. (*C*) Active phospho-Erk1/2 was immunoprecipitated from lysates of synchronized human Schwann cells by anti-phospho Erk1/2 antibody, and the resulting immunoprecipitate was then incubated with a fusion protein of Elk-1 transcription factor. Phosphorylation of Elk-1 at Ser-383, a major phosphorylation site of Erk1/2, was determined by phosho-Elk-1 antibody as a measure of kinase activity. (*D*) DNM of Erk2 inhibits *M. leprae*-induced S-phase entry. Infected human Schwann cells were transfected with Erk2/p44^{mapk} DNM T192A and vector alone, and cell cycle kinetics were analyzed by FACS. *, $P <$ 0.0001, Student's *t* test. (*Inset*) Cyclin D1 expression in transfected infected cells with vector alone (lane 1) and DNM T192A (lane 2) are shown. In all experiments, β-actin labeling is shown to indicate equal amount of proteins in each lane.

To elucidate the signaling mechanisms by which intracellular *M. leprae* induce MEK-independent Erk1/2 activation, 30-day-infected Schwann cells were serum-starved for 48 h with known inhibitors of major signaling pathways. We found that PKC pan-inhibitor (PKCI) bisindolyl maleimide-I (20 nM) (26), in the presence of MEKI and PI3KI, significantly blocked *M. leprae*-induced phosphorylation of Erk1/2 (Fig. 4*A*), suggesting a critical role of PKC in MEK-independent activation of Erk1/2.

The PKC family comprises ≈12 different isoforms that are phospholipid-dependent serine/threonine kinases and are broadly classified by their activation characteristics (27). To identify the PKC isoform(s) responsible for *M. leprae*-induced Erk1/2 activation, we used previously characterized DNMs of PKC isoforms (28). Infected cells transfected with DNM-PKCε, but not with other DNMs of PKC isoforms, significantly down-regulated Erk1/2 phosphorylation (Fig. 4*B*). This result was further confirmed by phospho-specific antibody to PKCε, which showed a strong activity in synchronized infected cells, compared with weak or no reaction in controls (Fig. 4*C*). Specificity of the former was confirmed by PKCI, which completely abolished PKCε phosphorylation (Fig. 4*C*). We also tested the activities of other phospho-specific antibodies to PKCα/βII, PKC∂, PKD/PKCμ, PKD/PKCμ, PKCθ, and PKCζ/λ, but none except PKCα/βII showed reactivity in human Schwann cells (data not shown). Because DNMs of PKCα and PKCβII had no effect on Erk1/2 (Fig. 4*B*), we concluded that PKCε is involved in *M. leprae*-induced Erk1/2 activation. Although PKC isoforms including PKCε have been shown to activate Erk1/2 by means of c-Raf and MEK (27–29), it is unknown whether PKC isoforms can activate Erk1/2 by MEK-independent pathways. Because Erk1/2 is not a substrate for PKCε (29), it is likely that MEK-independent Erk1/2 phosphorylation in infected Schwann cells is mediated by another signaling kinase(s) that serve as PKC-activated intermediate(s).

One of the kinase substrates of PKC is lymphoid cell kinase (Lck) p56Lck, a member of nonreceptor Src family tyrosine kinases, which was originally thought to express preferentially in lymphoid tissues (30). Lck is of special interest, because the recombinant form of murine Lck has been shown to phosphorylate Erk1/2 *in vitro* (31). Because Lck is a substrate for PKCε (32) and PKCε is involved in *M. leprae*-induced Erk1/2 phosphorylation (Fig. 4 *A–C*), we examined whether a pharmacological inhibitor of Src kinases, PP2, that blocks Lck (LckI) (33) could inhibit *M. leprae*-induced Erk1/2. When 30-day-infected cells were incubated with LckI (10 μM) in the presence of MEKI and PI3KI for 48 h, a significant reduction of *M. leprae*-induced phosphorylation of Erk1/2 was observed (Fig. 4*D*), suggesting a potential role of Lck in MEK- (and PI3K-) independent activation of Erk1/2 in human Schwann cells.

Because the expression and function of Lck in the peripheral nervous system is unknown, we first determined the expression of Lck in primary human Schwann cells and sciatic nerves. Whereas *Lck* gene expression in control and infected Schwann cells showed no difference in RT-PCR (Fig. 4*E*), a major difference was found in migration pattern of total Lck protein (nonphosphorylated) in SDS/PAGE (Fig. 4*F*). In synchronized control human Schwann cells, total Lck appeared as a slow-migrating ≈65-kDa band. However, in infected cells, Lck showed a prominent lower band at ≈60 kDa and a weaker 56-kDa band (Fig. 4*F Left*). Both 60-kDa and ≈65-kDa Lck proteins were detected in human sciatic nerve (Fig. 4*F Right*), suggesting that Lck in peripheral nerves exists in two configurations. Indeed, the configurational changes in Lck proteins in inactive (≈65-kDa) and active (≈60-kDa) stages of T cells have been shown and are known to occur by intramolecular interactions as well as phosphorylation and dephosphorylation (34, 35). In

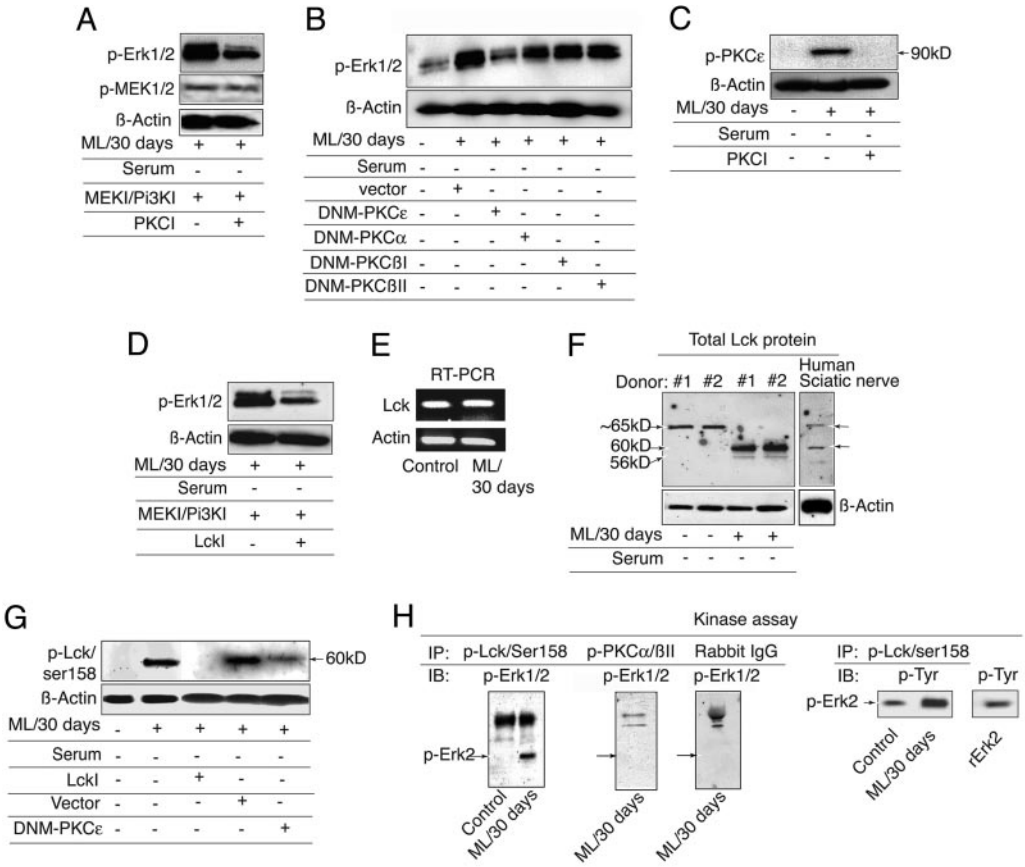

Fig. 4. *M. leprae*-induced Erk1/2 phosphorylation is mediated by p56Lck by means of a PKCε-dependent and MEK-independent pathway. (*A*) Thirty-day-infected Schwann cells were serum-starved for 48 h in the continuous presence of PI3KI and MEKI with or without PKCI bisindolylmaleimide. Erk1/2 and MEK1/2 phosphorylation was analyzed by immunoblotting with phospho-specific antibodies to Erk1/2 and MEK1/2, respectively. Protein loading was controlled by β-actin expression in all experiments. (*B* and *C*) Transient transfection of PKCε-DNM abrogated *M. leprae*-induced phosphorylation of Erk1/2. (*B*) Indicated PKC-DNM constructs were expressed in 30-day-infected Schwann cells and analyzed by Western blotting using antibody to phospho-Erk1/2. (*C*) Induction of *M. leprae*-induced phosphorylation of PKCε and its inhibition by PKCI. (*D*) LckI abrogated *M. leprae*-induced Erk1/2 activation in the presence of MEKI and PI3KI. Western blot analysis of infected cells incubated with MEKI and PI3KI in the absence and presence of LckI. (*E*) Expression of Lck in human primary Schwann cells (control and infected cells) was analyzed by RT-PCR (β-actin was used as a housekeeping gene). (*F*) (*Left*) Thirty-day-infected cells and controls from two individual donors (#1 and #2) were synchronized for 48 h, and the lysates were analyzed by Western blot using antibody to total Lck. (*Right*) Antibody activity to protein extract of human sciatic nerve is shown. (*G*) *M. leprae*-infected cells were incubated with LckI or transfected with DNM-PKCε or vector alone for 48 h without serum, and cell lysates were analyzed by Western blotting using phospho-Ser-158-specific Lck antibody. Note the phosphorylation at 60 kDa only. (*H*) Activated Lck-Ser-158 in infected human Schwann cells directly phosphorylates Erk2. (*Left*; arrows) Lysates of control and *M. leprae*-infected Schwann cells were immunoprecipitated with phospho-Lck-Ser-158 antibody, phospho-PKCα/βII antibody, or rabbit IgG, and precipitates were incubated with recombinant Erk2 in kinase buffer and then blotted with phospho-Erk1/2 antibody. (*Right*) The detection of phosphorylation of recombinant Erk2 by Lck-Ser-158 precipitated from Schwann cells using anti-phospho-Tyr antibody is shown. The same amount of recombinant Erk2 was incubated in kinase buffer without cell lysates and blotted with anti-phospho-tyrosine antibody. Note the Erk1/2 phosphorylation by activated Lck from infected Schwann cells.

Schwann cells, the observed migration difference in total Lck is likely due to similar configurational changes caused by *M. leprae*-induced cell activation.

Lck is regulated by phosphorylation on multiple residues, including Ser-158 in the SH2 domain (36). In T cell lines, specific PKC-mediated phosphorylation has been shown at Ser-158 of the active form of the Lck molecule (37). We tested whether Lck is phosphorylated at Ser-158. By using phospho-specific antibody to Lck/Ser-158, we detected phosphorylation only in the lysates of *M. leprae*-infected Schwann cells (Fig. 4*G*). Consistent with the total Lck protein expression pattern, phospho-Lck-Ser-158 was associated only with the 60-kDa band in infected cells (Fig. 4*G*). Both LckI and DNM-PKCε abolished phosphorylation of Lck-Ser-158, suggesting the role of PKCε in *M. leprae*-induced Lck activation (Fig. 4*G*). In contrast, unlike intracellular *M. leprae*, heregulin-β1, which activates Erk1/2 by means of the Ras/Raf/MEK pathway (24), failed to phosphorylate Lck-Ser-158 in Schwann cells (Fig. 9, which is published as supporting information on the PNAS web site).

To assess the role of Schwann cell Lck/Ser-158 in direct phosphorylation of Erk1/2, we performed an *in vitro* kinase assay with antibody to phospho-Lck/Ser-158. Phospho-Lck/Ser-158 immunoprecipitates from *M. leprae*-infected Schwann cells, but not from controls, directly phosphorylated Erk2 *in vitro* (Fig. 4*H*). These results were consistent with Schwann cells isolated from two different human donors (data not shown). In addition, we performed *in vitro* phosphorylation kinase assay using anti-phospho-Tyr antibody. Because Erk2 can be autophosphorylated on tyrosine residues in the presence of ATP (31), recombinant Erk2 was used as a positive control. Phospho-Lck/Ser-158 immunoprecipitated from the lysates of infected Schwann cells showed 2-fold increase in phosphorylation of Erk2 on tyrosine residues compared with autophosphorylated Erk2 (Fig. 4*H*). These data together suggest that phosphorylated Lck-Ser-158 in human Schwann cells serves as a direct activator of Erk1/2 independent of MEK1/2.

Although MEKIs and PI3KIs are known to block growth factor-induced Erk1/2 activation, nuclear cyclin D1, and cell cycle pro-

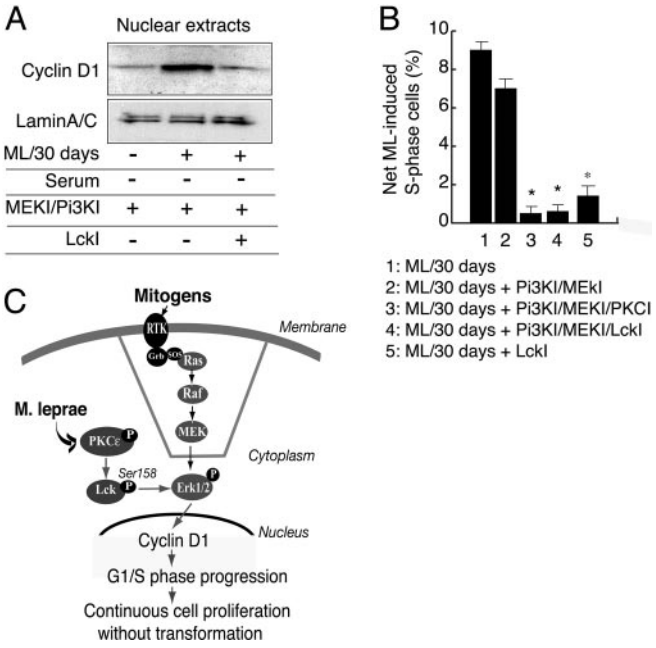

Fig. 5. Lck regulates *M. leprae*-induced nuclear accumulation of cyclin D1 and S-phase cells. (*A*) Thirty-day-infected human primary Schwann cells were serum-starved for 48 h in the continuous presence of MEKI and PI3KI with or without LckI, and immunoblots of the nuclear extracts were labeled with antibody to cyclin D1. Lamin A/C labeling is shown to indicate the purity of nuclear fraction and equal protein loading. (*B*) Cell cycle FACS analysis showing net *M. leprae*-induced S-phase cells (subtracted from synchronized control Schwann cells) in the continuous presence of MEKI and PI3KI with or without LckI. Data are presented from three independent experiments. *, $P < 0.001$, Student's *t* test. (*C*) A proposed model of Lck-mediated Erk1/2 activation and subsequent proliferation of human Schwann cells by intracellular *M. leprae* from inside the cells independent of the canonical Raf/MEK-dependent pathway.

gression (22, 24), these inhibitors did not affect *M. leprae*-induced Erk1/2 phosphorylation, nuclear cyclin D1, and the net S-phase cell population (Fig. 5 *A* and *B*). However, addition of LckI and PKCI to the above combination of inhibitors dramatically reduced the nuclear cyclin D1 and the net S-phase cell population (Fig. 5 *A* and *B*). Similar reduction was also observed when infected cells were incubated with LckI alone (Fig. 5*B*). In contrast, Lck inhibitor did not affect the net S-phase Schwann cell population induced by heregulin-β1 (Fig. 9*B*), which is consistent with the failure to induce phosphorylated Lck-Ser-158 by heregulin-β1 (Fig. 9*A*). These results show that a MEK-independent and Lck-dependent Erk1/2 signaling induced by intracellular *M. leprae* promotes G_1/S-phase transition of human Schwann cells, and this signaling pathway does not appear to operate in heregulin or extracellular mitogen-induced cell cycle progression (Fig. 5*C*).

Unlike Erk1/2 activation by the canonical Ras/Raf/MEK pathway, whose sustained activation leads to cell transformation (22), sustained activation of Lck-dependent Erk1/2 does not appear to cause cell transformation (Fig. 10, which is published as supporting information on the PNAS web site). Therefore, it is possible that intracellular *M. leprae*, by activating Lck-dependent Erk1/2, reduce the risk of tumorigenesis so that highly controlled cell propagation can be maintained during long-term infection. Considering the strict obligate intracellular parasitic nature of *M. leprae*, it is likely that this bacterium has evolved to subvert vital putative Schwann cell signaling pathways such as MEK-independent and Lck-dependent activation of Erk1/2 from inside the cell as an effective bacterial strategy for cell proliferation (Fig. 5*C*). This study, using *M. leprae* as an intracellular cue, also reveals a signaling mechanism for cell proliferation. The control of nuclear accumulation of cyclin D1 and G_1/S-phase progression by the activation of Erk1/2 by means of a MEK-independent and Lck-dependent signaling pathway was previously unknown and reflects a regulatory mechanism of glial cell proliferation that might play a role in dedifferentiation as well as nerve degeneration and regeneration.

We thank P. Wood for invaluable support, numerous discussions and advice on human Schwann cells, and provision of reagents; J. Krahenbuhl for providing *M. leprae*; E. C. Gotschlich and V. A. Fischetti for continuing support; I. B. Weinstein and J. W. Soh (both of Columbia University, New York) for DNMs of PKC isoforms; J. A. Diehl (University of Pennsylvania, Philadelphia) for DNM cyclin D1 constructs; and J. Pouyssegur (Centre National de la Recherche Scientifique–Unité Mixte de Recherche 6543, Nice, France) for the T192A Erk2 mutant; L. White and C. Eastby for assistance in isolation and preparation of Schwann cell cultures; W. Chow for technical assistance; and H. Shio for electron microscopy. We gratefully acknowledge the University of Miami Organ Procurement Organization for the provision of peripheral nerve tissues from adult human organ donors. This work was supported National Institute of Allergy and Infectious Diseases Grant R01 A145816 and National Institute of Neurological Disorders and Stroke Grant R01 NS45187 (to A.R.).

1. Bunge, R. P. (1994) *J. Neurol.* **242,** S19–S21.
2. Suter, U. & Scherer, S. S. (2003) *Nat. Rev. Neurosci.* **4,** 714–726.
3. Harrisingh, M. C. & Lloyd, A. C. (2004) *Cell Cycle* **3,** 1255–1258.
4. Chang, L. & Karin, M. (2001) *Nature* **410,** 37–40.
5. Vaudry, D., Stork, P. J. S., Lazarovici, P. & Eiden, L. E. (2002) *Science* **296,** 1648–1649.
6. Robinson, F. L., Whitehurst, A. W., Raman, M. & Cobb, M. H. (2002) *J. Biol. Chem.* **277,** 14844–14852.
7. Rambukkana, A., Zanazzi, G., Tapinos, N. & Salzer, J. L. (2002) *Science* **296,** 927–931.
8. Rambukkana, A. (2004) *Curr. Opin. Immunol.* **16,** 511–518.
9. Ng, V., Zanazzi, G., Timpl, R., Salzer, J. L., Brennan, P. J. & Rambukkana, A. (2000) *Cell* **103,** 511–524.
10. Stoner, G. L. (1979) *Lancet* **2,** 994–996.
11. Shetty, V. P., Antia, N. H. & Jacobs, J. M. (1988) *J. Neurol. Sci.* **88,** 115–131.
12. Johnson, P. C. (1997) in *Neuropathology*, eds. Davis, R. L. & Robertson, D. M. (Williams & Wilkins, Baltimore), 3rd Ed., pp. 1233–1323.
13. Brophy, P. J. (2002) *Science* **296,** 862–863.
14. WHO Wkly Epidemiol Rec. (2002) **77**.
15. Pardee, A. B. (1989) *Science* **246,** 603–608.
16. Fregien, N. L., White, L. A., Bunge, M. B. & Wood, P. M. (2004) *Glia* **49,** 24–35.
17. Truman, R. W. & Krahenbuhl, J. L. (2001) *Int. J. Lepr. Other Mycobact. Dis.* **69,** 1–12.
18. Bentley, C. A. & Lee, K. F. (2000) *J. Neurosci.* **20,** 7706–7715.
19. Sherr, C. J. (1995) *Trends Biochem. Sci.* **20,** 187–190.
20. Kim, H. A., Pomeroy, S. L., Whoriskey, W., Pawlitzky, I., Benowitz, L. I., Sicinski, P. P., Stiles, C. D. & Roberts T. M. (2000) *Neuron* **26,** 405–416.
21. Diehl, J. A. & Sherr, C. J. (1997) *Mol. Cell. Biol.* **17,** 7362–7374.
22. Roovers, K. & Assoian, R. K. (2000) *BioEssays* **22,** 818–826.
23. Pages, G., Lenormand, P., L'Allemain, G., Chambard, J. C., Meloche, S. & Pouyssegur, J. (1993) *Proc. Natl. Acad. Sci. USA* **90,** 8319–8323.
24. Harrisingh, M. C., Perez-Nadales, E., Parkinson, D. B., Malcolm, D. S., Mudge, A. W. & Lloyd, A. C. (2004) *EMBO J.* **23,** 3061–3071.
25. Cussac, D., Vidal, M., Leprince, C., Liu, W. Q., Cornille, F., Tiraboschi, G., Roques, B. P. & Garbay, C. (1999) *FASEB J.* **13,** 31–38.
26. Gassel, M., Breitenlechner, C. B., Konig, N., Huber, R., Engh, R. A. & Bossemeyer, D. (2004) *J. Biol. Chem.* **279,** 23679–23690.
27. Mellor, H. & Parker, P. J. (1998) *Biochem. J.* **332,** 281–292.
28. Soh, J.-W. & Weinstein, I. B. (2003) *J. Biol. Chem.* **278,** 34709–34716.
29. Ueffing, M., Lovric, J., Philipp, A., Mischak, H. & Kolch, W. (1997) *Oncogene* **15,** 2921–2927.
30. Molina, T. J., Perrot, J. Y., Penninger, J., Ramos, A., Audouin, J., Briand, P., Mak, T. W. & Diebold, J. (1998) *J. Immunol.* **160,** 3828–3834.
31. Ettehadieh, E., Sanghera, J. S., Pelech, S. L., Hess-Bienz, D., Watts, J., Shastri, N. & Aebersold, R. (1992) *Science* **255,** 853–855.
32. Ping, P., Song, C., Zhang, J., Guo, Y., Cao, X., Li, R. C., Wu, W., Vondriska, T. M., Pass, J. M., Tang, X. L., *et al.* (2002) *J. Clin. Invest.* **109,** 499–507.
33. Zhu, X., Kim, J. L., Newcomb, J. R., Rose, P. E., Stover, D. R., Toledo, L. M., Zhao, H. & Morgenstern, K. A. (1999) *Structure Fold. Des.* **7,** 651–661.
34. Salter, M. W. & Kalia, L. (2004) *Nat. Rev. Neurosci.* **5,** 317–328.
35. Kabouridis, P. S. (2003) *Biochem. J.* **371,** 907–915.
36. Reynolds, P. J., Hurley, T. R. & Sefton, B. M. (1992) *Oncogene* **7,** 1949–1955.
37. Soula, M., Rothhut, B., Camoin, L., Guillaume, J. L., Strosberg, D., Vorherr, T., Burn, P., Meggio, F., Fischer, S. & Fagard, R. (1993) *J. Biol. Chem.* **268,** 27420–27427.